High prevalence of low affinity peptide–MHC II tetramer–negative effectors during polyclonal CD4+ T cell responses

Joseph J. Sabatino Jr.,[1] Jun Huang,[2] Cheng Zhu,[2] and Brian D. Evavold[1]

[1]Department of Microbiology and Immunology, Emory University, Atlanta, GA 30322
[2]Wallace H. Coulter Department of Biomedical Engineering, Georgia Institute of Technology, Atlanta, GA 30332

T cell affinity for antigen initiates adaptive immunity. However, the contribution of low affinity cells to a response is unknown as it has not been possible to assess the entire affinity range of a polyclonal T cell repertoire. In this study, we used a highly sensitive two-dimensional binding assay to identify low affinity cells in polyclonal autoreactive and pathogen-reactive CD4+ T cell populations specific for myelin oligodendrocyte glycoprotein (MOG) and lymphocytic choriomeningitis virus (LCMV) antigens, respectively. Low affinity CD4+ T cells, below detection with peptide–major histocompatibility complex class II tetramers, were at least as frequent as high affinity responders and contributed significant effector cytokines in both primary antigen–specific responses. We further demonstrated that MOG- and LCMV-specific CD4+ T cells possessed similarly broad ranges in their affinities (>100-fold wide), only differing in the frequencies of low and high affinity cells. Thus, low as well as high affinity CD4+ T cells are critical effectors in autoimmune and pathogen-specific responses.

CORRESPONDENCE
Brian D. Evavold:
bevavol@emory.edu

Abbreviations used: 2D, two-dimensional; CNS, central nervous system; EAE, experimental autoimmune encephalomyelitis; GP, glycoprotein; LCMV, lymphocytic choriomeningitis virus; MOG, myelin oligodendrocyte glycoprotein; pMHC, peptide–MHC.

Determining the affinities of T cells in polyclonal responses is essential for understanding the outcome of cell-mediated immunity directed toward both foreign and self-antigens. The prevailing models of clonal selection and avidity maturation suggest that cells bearing the highest affinity TCRs for antigen are selectively expanded (Savage et al., 1999; Malherbe et al., 2004; Price et al., 2005), but the range in affinities of the T cells and the frequency of low affinity responders is unknown. The potential importance of low affinity T cells contributing to immunity is supported by the findings that monoclonal CD8+ T cells can proliferate to low affinity antigens (Zehn et al., 2009). In addition to foreign antigens, T cells specific for self-peptides that drive autoimmune disease could comprise another subset of low affinity cells as a result of tolerance mechanisms (Liu et al., 1995; Bouneaud et al., 2000; Zehn and Bevan, 2006). Although low affinity T cells may potentially contribute to responses to both foreign and self-antigens, it has been unclear how extensively low affinity T cells participate in polyclonal T cell responses where high affinity clonotypes are also present.

Insight into TCR affinity for antigen has been provided by three-dimensional and two-dimensional (2D) technologies, such as surface plasmon resonance, Förster resonance energy transfer, or micropipette-based assays (Alam and Gascoigne, 1998; Kersh et al., 1998; Huang et al., 2010; Huppa et al., 2010). However, to date, studies have only considered monoclonal TCRs and cannot reveal T cell frequency and breadth of affinities comprising an antigen-specific polyclonal population (Alam and Gascoigne, 1998; Kersh et al., 1998; Huang et al., 2010; Huppa et al., 2010). Peptide–MHC (pMHC) tetramers based on an enhanced TCR avidity via multivalent interactions provide the most valuable technique for detecting the frequency of antigen-specific T cells (Altman et al., 1996; Moon et al., 2007), yet the extent to which their limited avidity may preclude detection of low affinity

J. Huang's present address is Dept. of Microbiology and Immunology and Howard Hughes Medical Institute, Stanford University School of Medicine, Stanford, CA 94305.

The Rockefeller University Press $30.00
J. Exp. Med. Vol. 208 No. 1 81-90
www.jem.org/cgi/doi/10.1084/jem.20101574

The Journal of Experimental Medicine

T cells (Vollers and Stern, 2008; Wooldridge et al., 2009) is unknown. Developing sensitive and accurate measurements of T cell antigen reactivity is therefore of utmost importance to dissect the nature of the polyclonal T cell response.

Recently, we used a 2D-based affinity analysis, which measures TCR–pMHC binding in the cell membrane–anchored context (Huang et al., 2010; Huppa et al., 2010) to define a 1,000-fold range in affinities corresponding to response levels between a monoclonal $CD8^+$ T cell and a panel of altered peptide ligands (Huang et al., 2010). In this study, we harnessed the sensitivity of the 2D binding assay to define the antigen-specific frequencies and affinities of two polyclonal IA^b-restricted $CD4^+$ T cell populations specific for a self-antigen, myelin oligodendrocyte glycoprotein $(MOG)_{35–55}$, which induces experimental autoimmune encephalomyelitis (EAE; Mendel et al., 1995), and a foreign-antigen, glycoprotein $(GP)_{61–80}$, the dominant T helper epitope for lymphocytic choriomeningitis virus (LCMV; Oxenius et al., 1995; Homann et al., 2001). The 2D analysis revealed significantly larger frequencies of antigen-reactive $CD4^+$ T cells for both antigens as compared with pMHC II tetramers. Polyclonal T cell affinities were diverse, covering more than a 100-fold range of affinities, with a fraction identified as high affinity and tetramer positive and many as low affinity and tetramer negative. We defined the 2D affinity necessary for pMHC II tetramers to bind $CD4^+$ T cells and found that the low affinity tetramer-negative $CD4^+$ T cells contributed significantly to the effector cytokine response. The presence of low and high affinity T cells greatly expands the previously estimated frequencies of polyclonal $CD4^+$ T cell populations in peak effector responses (Homann et al., 2001; Moon et al., 2007; Williams et al., 2008).

RESULTS

pMHC II tetramers underestimate the frequencies of polyclonal $CD4^+$ T cells

Polyclonal antigen-reactive $CD4^+$ T cell frequencies are traditionally measured by pMHC II tetramers or functional experiments. To compare their responses, we generated in vitro polyclonal myelin- and viral-reactive $CD4^+$ T cells (see Materials and methods) and investigated the response with $MOG_{38–49}$-IA^b and $GP_{66–77}$-IA^b tetramers encompassing the respective core $CD4^+$ T cell epitopes (Fig. 1 A; Mendel et al., 1996; Homann et al., 2007; Sabatino et al., 2008). After 1 wk of stimulation in vitro, three times as many $GP_{61–80}$ $CD4^+$ T cells were identified by tetramer than $MOG_{35–55}$ $CD4^+$ T cells (32.4 ± 7.7% and 9.6 ± 2.8%, respectively; Fig. 1 B). Of interest, the tetramer-positive frequency of $MOG_{35–55}$ $CD4^+$ T cells remained relatively static (mean of 11.2 ± 2.4%) on repeated rounds of in vitro restimulation with antigen, whereas the tetramer-positive population specific for $GP_{61–80}$ $CD4^+$ T cells expanded to 59.2 ± 7.0% of the culture (Fig. 1 B). The tetramer data seemed strikingly low for the antigen-reactive $MOG_{35–55}$ $CD4^+$ T cells in particular and raised the possibility that the pMHC II tetramers were not detecting all antigen-specific $CD4^+$ T cells.

As an alternative measure of determining the frequency of antigen-specific $CD4^+$ T cells, we used the micropipette adhesion frequency assay, which measures the 2D interactions of receptor–ligand interactions (Chesla et al., 1998; Huang et al., 2007, 2010). In this assay, a single T cell was brought in and out of contact with an RBC coated with pMHC II to yield an adhesion frequency (the percentage of adhesions out of the total number of contacts, as described in Materials and methods). After stimulation with antigen for 1 wk in vitro, polyclonal $MOG_{35–55}$ and $GP_{61–80}$ $CD4^+$ T cells bound only with their respective antigens but not RBCs alone or irrelevant antigen (Fig. 1, C and D). 2D analysis revealed a range in adhesion frequencies, and antigen-specific $CD4^+$ T cell frequencies were determined by the percentage of T cell binding above irrelevant antigen background (>0.1; see $hCLIP_{103–117}$-IA^b in Fig. 1, C and D). Surprisingly, the majority of the $MOG_{35–55}$ $CD4^+$ T cells were antigen specific (69.2 ± 6.0%), eightfold higher than the tetramer-based frequencies measured in parallel (8.7 ± 1.6%; Fig. 1 E). Moreover, the micropipette assay identified a similar wide range in adhesion frequencies and a 2.5-fold increase over tetramer-positive $GP_{61–80}$ $CD4^+$ T cells (76.9 ± 3.4% vs. 30.9 ± 8.8%; Fig. 1 E). Thus, 2D binding demonstrated that most $CD4^+$ T cells in short-term cultures were antigen specific in contrast to the differences in frequency identified using pMHC II tetramer (Fig. 1 B).

pMHC II tetramer–negative $CD4^+$ T cells are low affinity but elicit robust effector responses

The degree of tetramer binding is critically dependent on TCR avidity (Crawford et al., 1998; Savage et al., 1999; Fassò et al., 2000; Slifka and Whitton, 2001), a parameter determined by intrinsic TCR affinity (Vollers and Stern, 2008; Wooldridge et al., 2009) and TCR levels (Crawford et al., 1998; Mallone et al., 2005). However, $MOG_{35–55}$ and $GP_{61–80}$ $CD4^+$ T cells expressed similar levels of surface TCRs (Fig. S1). To determine whether TCR affinity caused the deficiency in tetramer detection of polyclonal $CD4^+$ T cells, we used the micropipette-based assay to define 2D affinities. The effective 2D affinity (A_cK_a, in μm^4) of the T cell was derived from the adhesion frequency at equilibrium and expressed as a product of the two cells' contact areas (A_c) and 2D affinity (K_a). The 2D affinities were derived at 5 s because binding of both T cell populations reached equilibrium within seconds of contact (Fig. S2). The adhesion frequency was dependent on the molecular densities of TCR and pMHC and can potentially detect a dynamic range of affinities spanning six orders of magnitude (10^{-2}–10^{-8} μm^4; Huang et al., 2010), with lower affinity T cells requiring increased pMHC densities.

For comparable adhesion frequencies, $GP_{61–80}$ $CD4^+$ T cells (Fig. 1 D) required lower levels of antigen than many $MOG_{35–55}$ $CD4^+$ T cells (Fig. 1 C), which is indicative of overall higher affinity. Indeed, the population-averaged effective 2D affinity of $GP_{61–80}$ $CD4^+$ T cells was 26-fold higher than $MOG_{35–55}$ $CD4^+$ T cells (4.21 ± 1.48 × 10^{-4} μm^4 and 1.63 ± 0.48 × 10^{-5} μm^4, respectively; Fig. 2 A). Moreover, the effective 2D affinities paralleled the functional avidities (inverse of peptide

concentration for half-maximal proliferation, $1/EC_{50}$) as $GP_{61–80}$ $CD4^+$ T cells had a 61-fold higher functional avidity than $MOG_{35–55}$ $CD4^+$ T cells (Fig. 2 B).

pMHC tetramers provide a useful tool for separating the polyclonal $MOG_{35–55}$- and $GP_{61–80}$-specific $CD4^+$ T cells in two distinct populations based on reactivity to the tetramer (Fig. S3, A and B). Essentially all tetramer-positive $CD4^+$ T cells (>94%) were detected by 2D binding, showing high adhesion frequencies at low antigen densities (Fig. 2, C–E). Importantly, the majority of tetramer-negative $CD4^+$ T cells (68.6 ± 6.2% of $MOG_{35–55}$ and 75.0 ± 0.0% of $GP_{61–80}$) also bound to antigen in the micropipette assay (Fig. 2, C–E). Nevertheless, tetramer-negative $MOG_{35–55}$ and $GP_{61–80}$ $CD4^+$ T cells had lower effective 2D affinities ($6.67 \pm 3.14 \times 10^{-6}$ μm^4 and $8.36 \pm 2.49 \times 10^{-6}$ μm^4, respectively) than their tetramer-positive counterparts ($1.48 \pm 0.27 \times 10^{-4}$ μm^4 and $3.91 \pm 0.83 \times 10^{-4}$ μm^4, respectively; Fig. 2 F). Taken as a whole, all tetramer-positive $CD4^+$ T cells had an affinity $>1.10 \times 10^{-4}$ μm^4, and all tetramer-negative $CD4^+$ T cells had an affinity $<1.52 \times 10^{-5}$ μm^4 (Fig. 2 F). We were unable to more precisely pinpoint the affinity threshold for tetramer binding as the measurements were based on the $MOG_{35–55}$ and $GP_{61–80}$ experimental means and because the intermediate tetramer-binding $CD4^+$ T cells were excluded during cell sorting (Fig. S3, A and B). The presence of high and low affinity (henceforth broadly distinguished by the 2D affinity cutoff for tetramer binding) $MOG_{35–55}$ and $GP_{61–80}$ $CD4^+$ T cells indicated that both populations were comprised of T cell clonotypes possessing a large (>100-fold), mostly overlapping span of affinities (7.92×10^{-7} to 2.01×10^{-4} μm^4 for $MOG_{35–55}$ and 5.37×10^{-6} to 5.53×10^{-4} μm^4 for $GP_{61–80}$; Fig. 2 F).

Despite their lower affinity, the tetramer-negative $CD4^+$ T cells elicited robust effector functions as similar percentages of tetramer-positive and -negative $MOG_{35–55}$

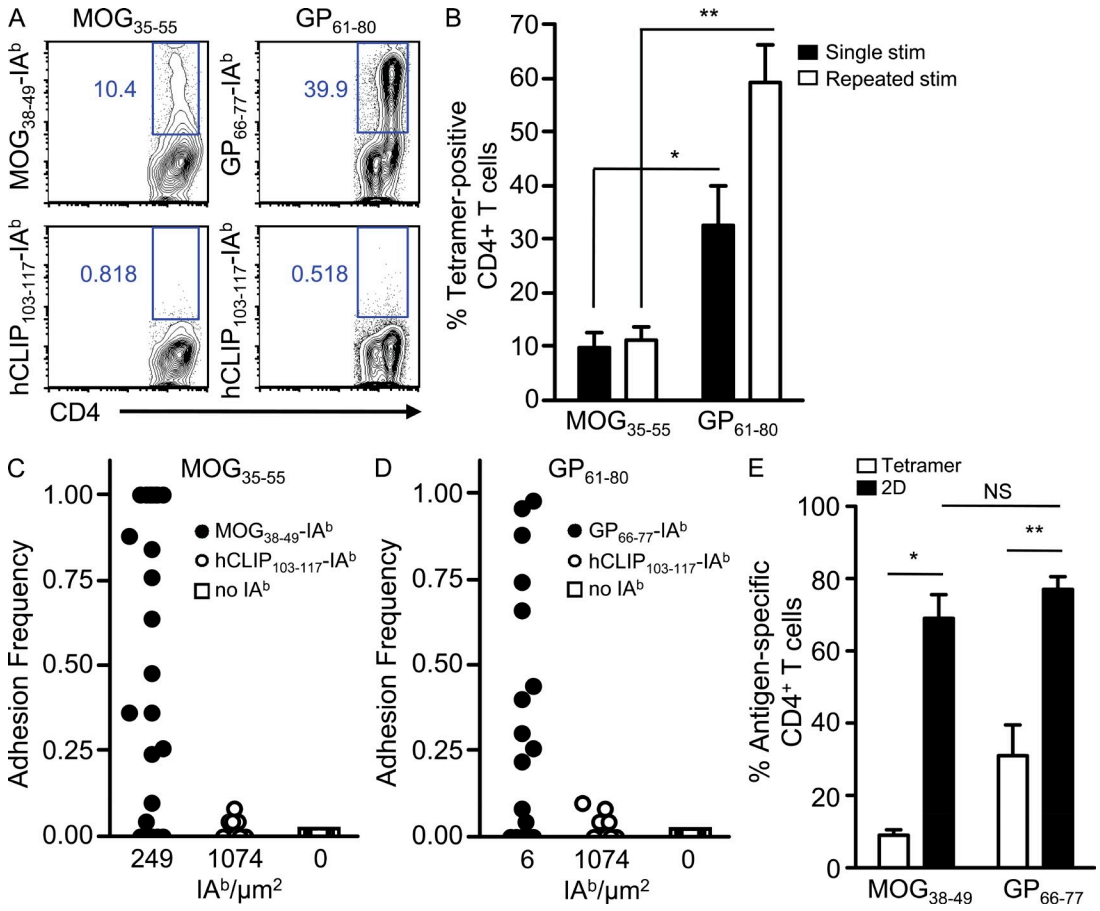

Figure 1. Tetramer versus 2D detection of polyclonal $MOG_{35–55}$ and $GP_{61–80}$ $CD4^+$ T cells. (A) Polyclonal $MOG_{35–55}$ and $GP_{61–80}$ $CD4^+$ T cells (after 1 wk in culture) were stained with the indicated tetramers in representative experiments. (B) $MOG_{35–55}$ and $GP_{61–80}$ $CD4^+$ T cells were restimulated with antigen for 1 wk (single stimulation [stim]) or for a consecutive 4 wk (repeated stimulation), and the mean percentages ± SEM of tetramer-positive $CD4^+$ T cells were measured in at least four independent experiments per group (*, P = 0.03; **, P = 0.0001). (C) Polyclonal $MOG_{35–55}$ $CD4^+$ T cells were tested for adhesion to the indicated concentrations (IA^b/square micrometer) of $MOG_{38–49}$-IA^b, $hCLIP_{103–117}$-IA^b, and no IA^b in a representative experiment. (D) Representative adhesion frequencies of polyclonal $GP_{61–80}$ $CD4^+$ T cells binding to $GP_{66–77}$-IA^b, $hCLIP_{103–117}$-IA^b, and no IA^b. (E) The mean frequency ± SEM of antigen-specific binding by tetramer and 2D analysis was measured in parallel for polyclonal $CD4^+$ T cells after 1 wk of passage in vitro (*, P = 0.0002; **, P = 0.0003). Data were based on four ($MOG_{35–55}$) and three ($GP_{61–80}$) independent experiments.

(54.6 ± 7.4% and 58.7 ± 19.1%, respectively) and $GP_{61–80}$ (81.4 ± 4.8% and 65.6 ± 5.7%, respectively) $CD4^+$ T cells produced TNF and/or IFN-γ after antigen stimulation (Fig. 2 G). Considering that tetramer-negative cells were not exclusively antigen reactive by 2D binding analysis, cytokine was produced at a higher frequency than in the tetramer-positive populations.

Low affinity tetramer-negative $CD4^+$ T cells in the central nervous system (CNS) dominate during peak EAE

An added strength of the micropipette assay is that its increased sensitivity to antigen allows assessment of ex vivo polyclonal T cell responses. $CD4^+$ T cells isolated from the CNS after EAE induction bound specifically to $MOG_{38–49}$-IA^b but not irrelevant antigen by both tetramer (Fig. 3 A) and 2D analysis (Fig. 3 B). The mean frequency of tetramer-positive $MOG_{35–55}$ $CD4^+$ T cells isolated from the CNS of mice with peak EAE symptoms was 8.2 ± 1.3% (Fig. 3 C), similar to previous findings (Korn et al., 2007; Sabatino et al., 2008). In parallel with the in vitro data, eightfold more CNS-infiltrating $MOG_{35–55}$ $CD4^+$ T cells were detected by 2D binding (63.6 ± 6.9%; Fig. 3 C). Moreover, the population-averaged effective 2D affinity of $MOG_{35–55}$-specific $CD4^+$ T cells from the CNS was 7.95 ± 2.77 × 10^{-6} μm⁴, which was comparable (2.1-fold lower) with the in vitro analysis (Fig. 2 A). This affinity level explains the low degree of tetramer staining as it was below the threshold for tetramer binding (Fig. 2 F). Thus, the majority of

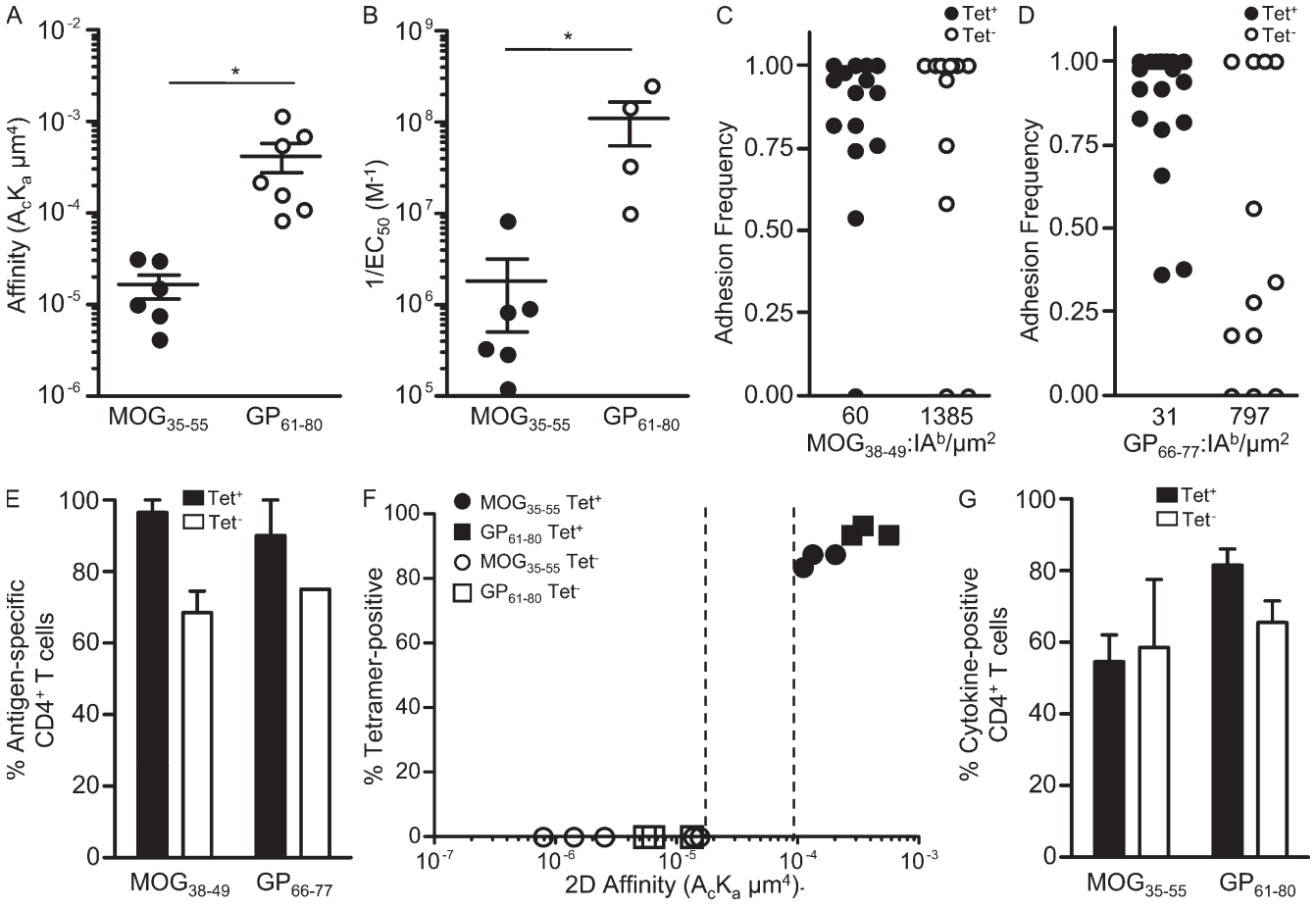

Figure 2. 2D affinity and antigen specificity of tetramer-positive and -negative $CD4^+$ T cells. (A) The mean affinities ± SEM of polyclonal $MOG_{35–55}$ and $GP_{61–80}$ $CD4^+$ T cells were based on 62 $MOG_{35–55}$ $CD4^+$ T cells (six independent experiments) and 54 $GP_{61–80}$ $CD4^+$ T cells (three independent experiments encompassing seven different antigen densities; *, P = 0.03). (B) The mean ± SEM functional avidities (1/EC_{50}, based on proliferation) of polyclonal $MOG_{35–55}$ (1.8 ± 1.3 × 10^6 M^{-1}) and $GP_{61–80}$ (1.1 ± 0.6 × 10^8 M^{-1}) $CD4^+$ T cells were based on six and four independent experiments, respectively (*, P = 0.04). (C and D) Representative adhesion frequencies of tetramer-positive and -negative sorted $MOG_{35–55}$ (C) and $GP_{61–80}$ (D) $CD4^+$ T cells were performed at the indicated antigen densities. (E) The mean percentage ± SEM of antigen-specific 2D binding of tetramer-positive and -negative $MOG_{35–55}$ and $GP_{61–80}$ $CD4^+$ T cells was based on three ($MOG_{35–55}$) and two ($GP_{61–80}$) independent experiments. (F) The mean 2D affinities of tetramer-positive and -negative $MOG_{35–55}$ and $GP_{61–80}$ $CD4^+$ T cells were based on at least three independent experiments per group. The affinity threshold for tetramer binding is shown by the dotted lines, representing the lowest affinity for tetramer-positive $CD4^+$ T cells (>1.10^{-4} μm⁴) and the highest affinity for tetramer-negative $CD4^+$ T cells (<1.52 x 10^{-5} μm⁴). (G) The mean percentage ± SEM of cytokine-producing (IFN-γ and TNF) tetramer-positive and -negative $MOG_{35–55}$ and $GP_{61–80}$ $CD4^+$ T cells was based on three and two independent experiments, respectively.

$CD4^+$ T cells penetrating the CNS at the peak of EAE were in fact $MOG_{35–55}$ specific.

The presence of a large frequency of predominantly tetramer-negative $MOG_{35–55}$ $CD4^+$ T cells in the CNS during EAE suggested that low affinity myelin-reactive $CD4^+$ T cells contributed to disease pathogenesis. To define the effector function of low affinity $MOG_{35–55}$ $CD4^+$ T cells in the CNS, we isolated $CD4^+$ T cells from the CNS at the peak of EAE and assessed their ability to produce IFN-γ and TNF (Fig. 3 D). Approximately 2.4-fold more $CD4^+$ T cells produced cytokine in response to $MOG_{35–55}$ peptide stimulation than were detected by tetramer (19.0 ± 3.6% vs. 8.0 ± 0.7%, in parallel experiments; Fig. 3 E). Because not all antigen-specific $CD4^+$ T cells produced cytokine (Fig. 2 G) and because the tetramer-negative $MOG_{35–55}$ $CD4^+$ T cells outnumbered their tetramer-positive counterparts by ∼8:1 (Fig. 3 C), this indicated that the majority of proinflammatory cytokine-secreting $MOG_{35–55}$-specific $CD4^+$ T cells were of low affinity.

High frequency of LCMV-specific tetramer-negative $CD4^+$ T cells at the peak effector phase

To measure ex vivo antiviral $CD4^+$ T cells, we analyzed the $GP_{61–80}$ LCMV-specific $CD4^+$ T cell response at its peak, 8 d postinfection with LCMV Armstrong (Homann et al., 2001; Whitmire et al., 2006). $CD4^+$ T cells from the spleen bound specifically to $GP_{66–77}$-IA^b by tetramer (Fig. 4 A) and 2D analysis (Fig. 4 B). Interestingly, although 8.9 ± 0.4% of $CD4^+$ T cells from the spleen were detected by pMHC II tetramer, 33.7 ± 4.8% were in fact $GP_{61–80}$ specific by 2D adhesion analysis (Fig. 4 C). This frequency closely matched the percentage (37.2%) of $CD44^+$ $CD4^+$ T cells that were induced by LCMV at day 8 postinfection. The mean effective 2D affinities (1.65 ± 0.79 × 10^{-4} μm⁴) of the $GP_{61–80}$ $CD4^+$ T cells in LCMV infection were again 2.6-fold less than in vitro $GP_{61–80}$ $CD4^+$ T cells (Fig. 2 A). Although viral-specific $CD4^+$ T cells displayed an overall higher 2D affinity than myelin-specific $CD4^+$ T cells, pMHC II tetramer nonetheless underestimated their frequency by fourfold.

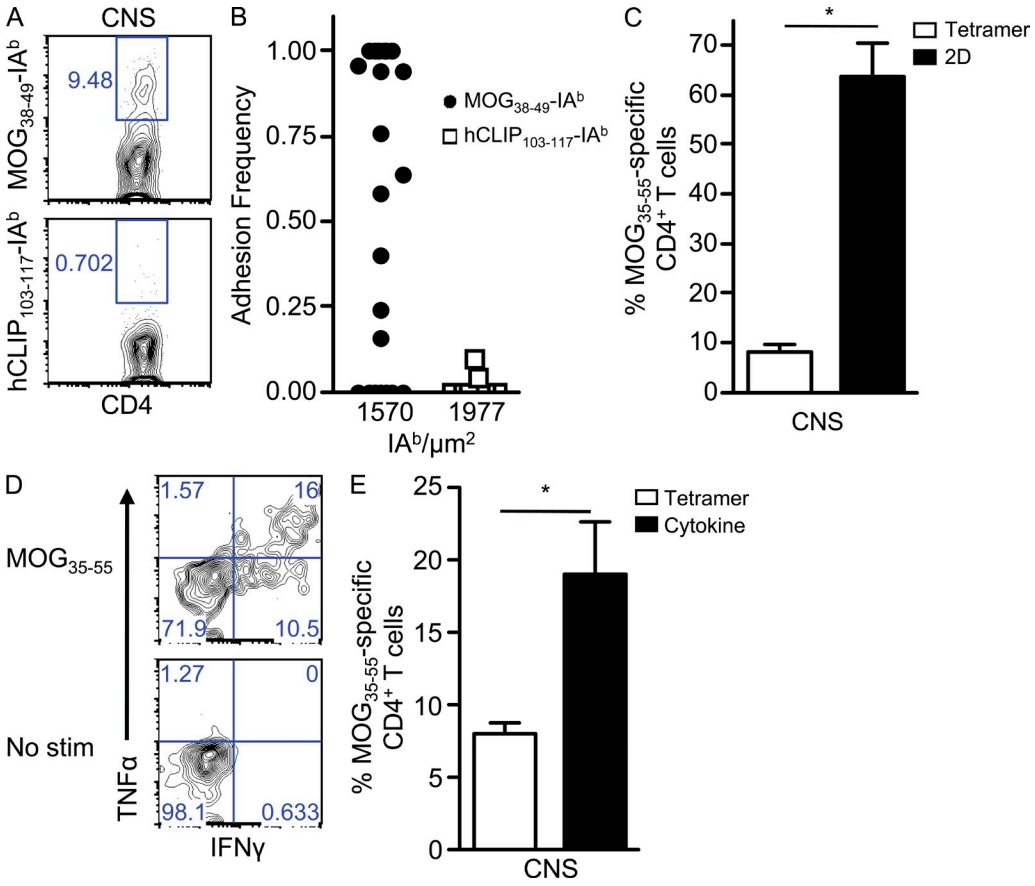

Figure 3. Dominance of proinflammatory low affinity myelin-reactive $CD4^+$ T cells during EAE. (A and B) Representative tetramer (A) and 2D binding (B) of CNS-infiltrating $CD4^+$ T cells to $MOG_{38–49}$-IA^b and $hCLIP_{103–117}$-IA^b. (C) The mean frequency ± SEM of $MOG_{35–55}$-specific binding by tetramer and 2D analysis was based on three experiments performed in parallel, and CNS tissue was pooled together from 6–10 mice per experiment (*, P = 0.004). (D) Representative frequency of cytokine-producing (IFN-γ and TNF) $CD4^+$ T cells isolated from the CNS during acute EAE after stimulation with $MOG_{35–55}$ or no peptide (no stimulation [stim]). (E) The mean percentage ± SEM of CNS-infiltrating $MOG_{35–55}$ $CD4^+$ T cells was compared in parallel by $MOG_{38–49}$-IA^b tetramer and the percentage producing cytokine (IFN-γ and TNF) upon stimulation with $MOG_{35–55}$ (no stimulation background subtracted) from two independent experiments (CNS tissue pooled from 12–24 mice; *, P = 0.04).

To determine the contribution of low affinity T cells to overall effector function, splenocytes 8 d postinfection were sorted into $GP_{66–77}$-IA^b tetramer-positive and -negative $CD4^+$ T cells and assessed for cytokine production (TNF and IFN-γ) in response to $GP_{61–80}$ stimulation. In the absence of the $GP_{66–77}$-IA^b tetramer-positive $CD4^+$ T cells, the tetramer-negative population produced approximately half of the total cytokines detected at all doses of antigen (Fig. 4 D). There was no significant difference (P = 0.80) in the EC_{50} values for cytokine production from the LCMV tetramer-positive or -negative or intact (i.e., unsorted) $CD44^+$ $CD4^+$ T cell populations (Fig. 4 E). The data were displayed as a percentage of maximal response because essentially all of the tetramer-positive $CD4^+$ T cells were antigen reactive, whereas LCMV-specific $CD4^+$ T cells comprised a third or less of the total and tetramer-negative $CD4^+$ T cell populations. Thus, LCMV-specific, tetramer-negative $CD4^+$ T cells were present at a greater frequency than the tetramer-positive population and produced a substantial fraction of the overall effector cytokine response.

DISCUSSION

T cells mount a response against antigens that is typically clonally diverse, but often experiments analyzing cell-mediated immunity must use monoclonal cells to facilitate analysis of cell fate, location, frequency, and affinity. Biophysical analyses of T cell affinity have almost exclusively focused on a single TCR species complicating extrapolation to polyclonal populations. The focus on one clonal TCR very likely limits our understanding into the range of affinities comprising the antigen-activated T cell population and prevents investigation into the distinct possibility that low affinity T cells appreciably participate in immunity (Gronski et al., 2004; Zehn et al., 2009). In this study, we applied a micropipette-based 2D binding technology to measure the affinities and frequencies of polyclonal $CD4^+$ T cells by taking advantage of its capability over other measures to resolve low affinity monoclonal TCR–pMHC interactions (Huang et al., 2010). Beyond allowing analysis of polyclonal $CD4^+$ T cell affinity, 2D analysis revealed significantly larger numbers of antigen-specific $CD4^+$ T cells than can be quantified using pMHC II tetramers.

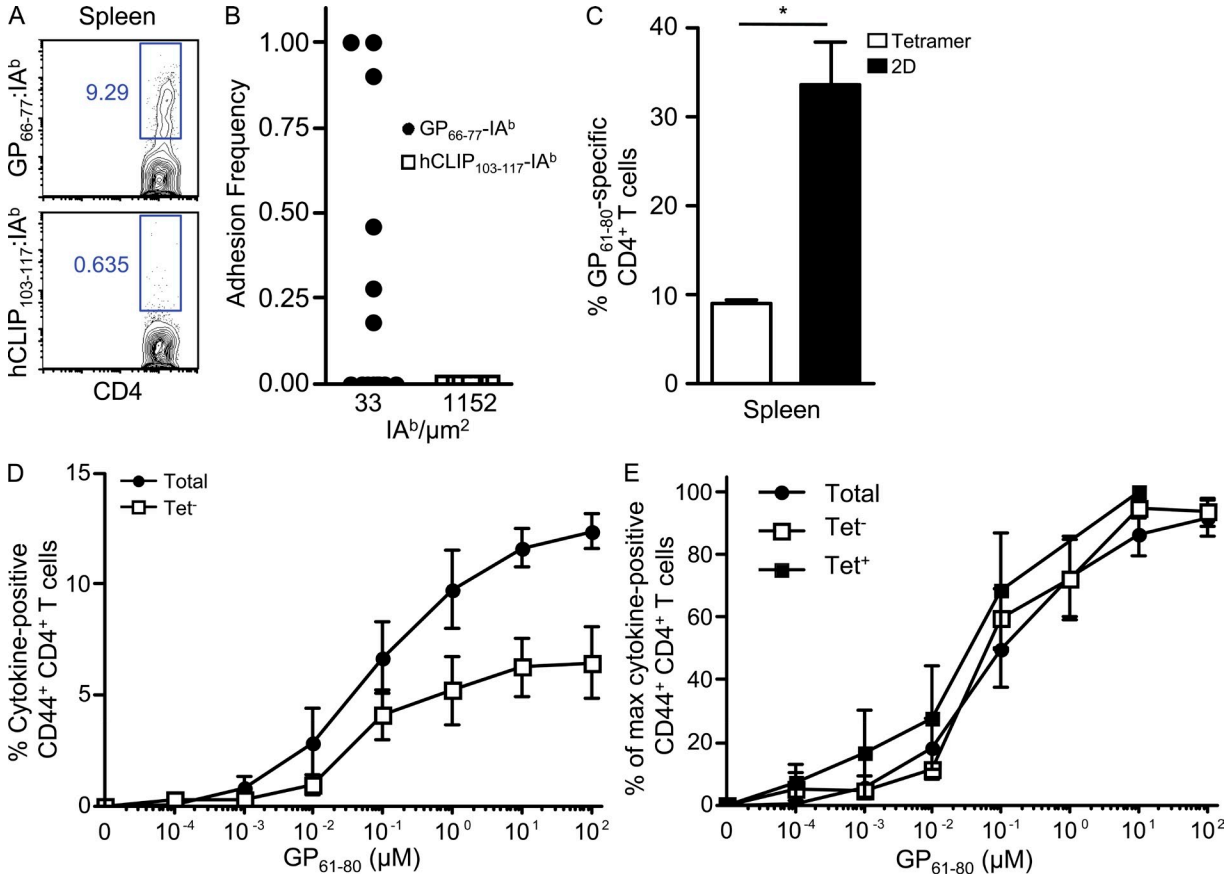

Figure 4. Low affinity viral-specific $CD4^+$ T cells contribute significant effector responses during LCMV infection. (A and B) Representative tetramer (A) and 2D binding (B) of $CD4^+$ T cells from the spleen at day 8 LCMV to $GP_{66–77}$-IA^b and $hCLIP_{103–117}$-IA^b. (C) The mean frequency ± SEM of $GP_{61–80}$ $CD4^+$ T cells in the spleen during LCMV infection by tetramer and 2D analysis was performed in parallel in three independent experiments (two spleens pooled per experiment; *, P = 0.007). (D and E) At day 8 postinfection, total $CD44^+$ $CD4^+$, tetramer-positive $CD44^+$ $CD4^+$, or tetramer-negative $CD44^+$ $CD4^+$ T cells were stimulated with the indicated concentrations of $GP_{61–80}$ peptide, and the mean total ± SEM percentages of (D) and percentage of maximal ± SEM (E) cytokine-producing (IFN-γ and TNF) cells were assessed in four independent experiments (two to four spleens pooled per experiment).

pMHC tetramers provide an important technique for quantifying the immune response and can be used to define a polyclonal population of antigen-specific precursor or effector T cells, yet their limited avidity inherently restricts the range of affinities that can be analyzed. Indeed, the ex vivo $GP_{61–80}$ and $MOG_{35–55}$ $CD4^+$ T cell populations were four- and eightfold larger, respectively, than indicated by pMHC II tetramer. These differences between $GP_{61–80}$- and $MOG_{35–55}$-specific $CD4^+$ T cells as prototypical foreign- and self-specific responses mirror other studies in which $CD4^+$ T cells specific for foreign antigens (Homann et al., 2001; Moon et al., 2007) were more prevalent and easier to detect by tetramer than those specific for self-antigens (Gebe et al., 2003; Bischof et al., 2004; Falta et al., 2005; Korn et al., 2007). Regardless, pMHC II tetramer underestimated the frequency of $MOG_{35–55}$ and $GP_{61–80}$ $CD4^+$ T cells, as the pMHC II tetramer staining was only accurate to the extent that the underlying T cell responses were dominated by high affinity T cells. It is currently unknown whether pMHC II tetramers are a sufficient surrogate for tracking $CD4^+$ T cell responses. Interestingly, the $CD4^+$ T cells possessed similar overlapping distributions of low to high affinities for $MOG_{35–55}$ and $GP_{61–80}$. In fact, the effective 2D affinities of tetramer-negative or -positive cells were essentially the same regardless of T cell specificity for the myelin or viral antigens.

Previous work in $CD4^+$ T cells suggested rapid dominance of high affinity T cell clonotypes (Savage et al., 1999; Malherbe et al., 2004), yet these studies were based on pMHC II tetramer measurements. By including tetramer-negative $CD4^+$ T cells in our analysis, a 2D affinity range >100-fold wide was present at the peak immune response for both foreign and self-antigens. This indicates heterogeneity in TCR affinity regardless of antigen specificity during the polyclonal primary immune responses and may raise issues over the accuracy that a monoclonal T cell population possessing a single affinity completely reflects the ongoing immune processes. For example, monoclonal $MOG_{35–55}$-specific $CD4^+$ T cells may differ because of limited affinity diversity from polyclonal populations of cells. In fact, the $MOG_{35–55}$-specific 2D2 TCR transgenic, while a valuable model to highlight many features associated with demyelinating disease, generates a variant form of EAE (Bettelli et al., 2003, 2006; Wasserman and Evavold, 2008). Interestingly, 2D2 T cells are undetectable by the MOG-IA^b tetramer (unpublished data) yet pathogenic (Bettelli et al., 2003, Wasserman and Evavold, 2008), demonstrating that low affinity $MOG_{35–55}$ $CD4^+$ T cells can induce EAE. We are in the process of carrying out experiments to test the concept that autoimmune disease outcome relates to the affinity range and diversity of the response.

Although our experiments do not directly address the effect of thymocyte negative selection or peripheral events in shaping T cell affinity as we examined expanded cell populations, the mere presence of high affinity $MOG_{35–55}$ $CD4^+$ T cells suggests that their clonal deletion was absent or incomplete. Moreover, the stable existence of high affinity self-reactive T cells refines our ideas on clonal selection and avidity maturation (Savage et al., 1999; Malherbe et al., 2004; Price et al., 2005) because they did not dominate over their low affinity counterparts at the peak of the primary immune response or on extended culture in vitro. Similarly, the affinities of the $GP_{61–80}$ $CD4^+$ T cells were broadly distributed and contained a significant population of low affinity LCMV-reactive $CD4^+$ T cells detectable by 2D binding but not pMHC II tetramer. The presence of low affinity $GP_{61–80}$ $CD4^+$ T cells further demonstrates a lack of exclusive dominance by higher affinity T cell clones during a primary pathogen-specific response or on successive selective cycles with antigen in vitro. Thus, it is appears that breadth in affinity is maintained within a $CD4^+$ polyclonal population, at least during the peak effector response.

To detect antigen-reactive $CD4^+$ T cells by 2D analysis, the T cells had to recognize and proliferate to antigen encountered in vivo, regardless of low or high affinity. Moreover, we identified low and high affinity T cells within the immune-relevant tissues. In the case of the CNS, its immune privileged status would be presumed to allow primarily the myelin-reactive $CD4^+$ T cells, which we demonstrated by 2D analysis. Further demonstrating the active role of tetramer-negative $CD4^+$ T cells in immunity was their ability to contribute substantially to the overall cytokine responses. We found that the relative cytokine contribution of tetramer-negative $CD4^+$ T cells was approximately equal to or greater than the high affinity responders in viral immunity. Moreover, the high and low affinity LCMV-specific $CD4^+$ T cells had the same functional avidities despite their inherent 2D affinity differences, which is likely the result of tuning to the same level of antigen in vivo (Grossman and Paul, 1992; Slifka and Whitton, 2001). The prevalence of cytokine-positive low affinity myelin-reactive $CD4^+$ T cells clearly outnumbered the small frequency of tetramer-positive $MOG_{35–55}$ $CD4^+$ T cells, demonstrating the importance of low affinity effectors in CNS autoimmunity.

However, cytokine analyses of $CD4^+$ T cell effector function are limited because we and others have shown that not all antigen-specific $CD4^+$ T cells produce cytokine (Weaver et al., 1998; Bettelli et al., 2006; Whitmire et al., 2006; Williams et al., 2008). Because tetramer and intracellular cytokine staining usually cannot be performed concurrently, they are often performed in parallel. Although we confirm in this study what others have shown, that pMHC II tetramer and cytokine responses were approximately equal in LCMV infection (Homann et al., 2001; Williams et al., 2008), we demonstrated that the tetramer-negative $CD4^+$ T cells were major contributors to the effector cytokine response. Thus, an identical frequency of antigen-specific $CD4^+$ T cells by cytokine and tetramer is fortuitous as opposed to being an indication that they are the same high affinity responding T cell population.

In conclusion, 2D analysis resolved the affinity of polyclonal T cell responses and revealed that low affinity $CD4^+$ T cells participated during autoimmunity and viral infection, although they were accompanied by high affinity counterparts in both cases. Characterization of low affinity cell frequency

therefore allows for increased understanding of the polyclonal T cell response and ultimately enables defining how the affinity range impacts the extent of cell-mediated immunity.

MATERIALS AND METHODS

Mice. C57BL/6 mice were purchased from the National Cancer Institute and housed in an Emory University Department of Animal Resources facility (Atlanta, GA) and used in accordance with an Institutional Animal Care and Use Committee–approved protocol.

Peptides. $MOG_{35–55}$ (MEVGWYRSPFSRVVHLYRNGK) and $GP_{61–80}$ (GLNGPDIYKGVYQFKSVEFD) peptides were synthesized on a Prelude peptide synthesizer (Protein Technologies, Inc.).

Cells and reagents. All cells were cultured in RPMI 1640, supplemented with 10% FBS, 2 mM L-glutamine, 0.01 M Hepes, 100 μg/ml gentamicin (all Mediatech), and 20 μM 2-ME (Sigma-Aldrich). Polyclonal T cell lines were generated by footpad priming 2–3-mo-old male mice with 100 μg of the indicated peptide emulsified in CFA containing 1 mg/ml heat-killed *Mycobacterium tuberculosis*. Draining lymph nodes were harvested 10–14 d later and stimulated for 1 wk with 1 μM of the priming peptide and IL-2. Cells were CD4 purified by positive selection microbeads (Miltenyi Biotec). $CD4^+$ T cells were restimulated weekly with irradiated syngeneic splenocytes (3,000 rad) and 1 μM peptide and IL-2. Proliferation was measured by [^{3}H]thymidine incorporation as previously described (Sabatino et al., 2008).

Tetramer and cell surface staining. $MOG_{38–49}$-IA^b (generated from a previously described construct; Sabatino et al., 2008), $GP_{66–77}$-IA^b, and $hCLIP_{103–117}$-IA^b monomers and tetramers were provided by the National Institute of Allergy and Infectious Diseases Tetramer Core Facility at Emory University. $CD4^+$ T cells were incubated with 4 μg/ml $MOG_{38–49}$-IA^b (8–20 h), $GP_{66–77}$-IA^b tetramers (3–4 h), or $hCLIP_{103–117}$-IA^b in complete RPMI at 37°C. The following antibodies and stains were used for analysis: CD4 (RM4.5), CD8-α (53–6.7), B220 (RA3-6B2), CD11b (M1/70), 7-AAD (all BD), TCR-β (H57-597; eBioscience), and MHC II (M5/114.15.2; BioLegend). All flow cytometric analysis was performed on a FACSCalibur (BD), and data were analyzed using FlowJo (Tree Star, Inc.). Cell sorting on a FACSAria II was performed by the Emory University Flow Cytometry Core.

Intracellular cytokine detection. $CD4^+$ T cells were stimulated with IA^b-expressing fibroblasts (clone FT7.1C6, (Ronchese et al., 1987) and the indicated concentrations of peptide for 5 h at 37°C in the presence of 10 μg/ml brefeldin A. T cells were stained with CD4, fixed/permeabilized using the Fix and Perm Cell Permeabilization kit (Invitrogen), and stained for intracellular IFN-γ (XMG1.2) and TNF (MP6-XT22; both BD). To calculate the percentage of maximal cytokine production, the percentage of cytokine-producing $CD44^+$ $CD4^+$ T cells at a given concentration of peptide stimulation was divided by the maximal percentage of cytokine-producing $CD44^+$ $CD4^+$ T cells that was elicited at any peptide stimulation.

Ex vivo $CD4^+$ T cell analysis in EAE and LCMV. EAE was induced in 6–8-wk-old female mice as previously described (Ford and Evavold, 2003; Sabatino et al., 2008). For LCMV infection, 2–3-mo-old male mice were injected i.p. with 2×10^5 pfu LCMV Armstrong (provided by R. Ahmed, Emory University; Murali-Krishna et al., 1998). At the time of analysis, all mice were euthanized and perfused with saline. At 21 d postimmunization for EAE, brains and spinal cords were harvested and pooled together from 8–10 mice per experiment. Infiltrating mononuclear cells from the CNS were isolated over Percoll (Sigma-Aldrich). 8 d post-LCMV infection, spleens were harvested and pooled together from two to four mice per experiment. All cells were CD4 purified by positive selection microbeads as described in Cells and reagents to 90–95% purity. Cells were stained with tetramer as described in Tetramer and cell surface staining and washed and stained with CD4 FITC and a dump channel cocktail of CD8-α, B220, CD11b (all PerCP), and 7-AAD. For assessing the cytokine response in LCMV, $CD4^+$ T cells purified from the spleen at day 8 postinfection were sorted into $GP_{66–77}$-IA^b tetramer-positive and -negative $CD44^+$ $CD4^+$ T cells.

Cell preparation for micropipette adhesion frequency assay. Human RBCs were isolated in accordance with the Institutional Review Board at the Georgia Institute of Technology and prepared as previously described (Huang et al., 2007, 2010). RBCs coated with various concentrations of Biotin-X-NHS (EMD) were coated with 0.5 mg/ml streptavidin (Thermo Fisher Scientific), followed by 1–2 μg of pMHC II monomer. The pMHC-coated RBCs were stained with anti-MHC II FITC antibody, and T cells were stained with anti-TCR FITC antibody. The site densities of IA^b monomers per RBC and TCRs per T cell were derived using FITC MESF beads (Bangs Laboratories) as previously described (Huang et al., 2007, 2010) and normalized for the F/P ratios of the antibodies.

2D TCR affinity analysis. The details of the micropipette adhesion frequency assay are described in detail elsewhere (Huang et al., 2007, 2010). In brief, a pMHC-coated RBC and T cell were placed on apposing micropipettes and brought into contact by micromanipulation for a controlled contact area (A_c) and time (t). The T cell was retracted at the end of the contact period, and the presence of adhesion (indicating TCR–pMHC ligation) was observed microscopically by elongation of the RBC membrane. This contact–retraction cycle was performed 50 times per T cell–RBC pair to calculate an adhesion frequency (P_a). The contact area was kept constant for all experiments so it would not affect the affinity comparison. For each experiment, a mean P_a was calculated based only on T cells that bound specifically to antigen. The population-averaged 2D affinity (A_cK_a) using the mean P_a at equilibrium (where $t \rightarrow \infty$) was calculated using the following equation: $A_cK_a = \ln[1-P_a(\infty)]/(m_rm_l)$, where m_r and m_l reflect the receptor (TCR) and ligand (pMHC) densities, respectively.

Statistical analysis. Statistical analyses were performed using Prism 4 (GraphPad Software, Inc.). Two-way Student's t tests were used for all statistical comparisons, except in the comparison of the EC_{50} values of cytokine-producing $CD4^+$ T cells in LCMV, where a one-way analysis of variance was used.

Online supplemental material. Fig. S1 shows that $MOG_{35–55}$ and $GP_{61–80}$ $CD4^+$ T cells do not differ in their TCR levels. Fig. S2 demonstrates that the adhesion frequencies of polyclonal $MOG_{35–55}$ and $GP_{61–80}$ $CD4^+$ T cells reach steady-state within several seconds of binding. Fig. S3 shows the representative purities of tetramer-positive and -negative $MOG_{35–55}$ and $GP_{61–80}$ $CD4^+$ T cells after cell sorting. Online supplemental material is available at http://www.jem.org/cgi/content/full/jem.20101574/DC1.

We thank A. Stout and J. Shires for preparation of the pMHC II monomers and tetramers, R. Karaffa and S. Durham for assistance with tetramer-based cell sorting experiments, and L. Edwards and M. Ford for their helpful comments.

This work was supported by National Multiple Sclerosis Society grant RG4047-A-3 and National Institutes of Health grants NS071518 (to B.D. Evavold) and AI38282 and AI060799 (to C. Zhu).

The authors have no conflicting financial interests.

Submitted: 3 August 2010
Accepted: 10 December 2010

REFERENCES

Alam, S.M., and N.R. Gascoigne. 1998. Posttranslational regulation of TCR Valpha allelic exclusion during T cell differentiation. *J. Immunol.* 160:3883–3890.

Altman, J.D., P.A.H. Moss, P.J.R. Goulder, D.H. Barouch, M.G. McHeyzer-Williams, J.I. Bell, A.J. McMichael, and M.M. Davis. 1996. Phenotypic analysis of antigen-specific T lymphocytes. *Science.* 274:94–96. doi:10.1126/science.274.5284.94

Bettelli, E., M. Pagany, H.L. Weiner, C. Linington, R.A. Sobel, and V.K. Kuchroo. 2003. Myelin oligodendrocyte glycoprotein–specific T cell receptor transgenic mice develop spontaneous autoimmune optic neuritis. *J. Exp. Med.* 197:1073–1081. doi:10.1084/jem.20021603

Bettelli, E., Y. Carrier, W. Gao, T. Korn, T.B. Strom, M. Oukka, H.L. Weiner, and V.K. Kuchroo. 2006. Reciprocal developmental pathways for the generation of pathogenic effector TH17 and regulatory T cells. *Nature*. 441:235–238. doi:10.1038/nature04753

Bischof, F., M. Hofmann, T.N. Schumacher, F.A. Vyth-Dreese, R. Weissert, H. Schild, A.M. Kruisbeek, and A. Melms. 2004. Analysis of autoreactive CD4 T cells in experimental autoimmune encephalomyelitis after primary and secondary challenge using MHC class II tetramers. *J. Immunol.* 172:2878–2884.

Bouneaud, C., P. Kourilsky, and P. Bousso. 2000. Impact of negative selection on the T cell repertoire reactive to a self-peptide: a large fraction of T cell clones escapes clonal deletion. *Immunity*. 13:829–840. doi:10.1016/S1074-7613(00)00080-7

Chesla, S.E., P. Selvaraj, and C. Zhu. 1998. Measuring two-dimensional receptor-ligand binding kinetics by micropipette. *Biophys. J.* 75:1553–1572. doi:10.1016/S0006-3495(98)74074-3

Crawford, F., H. Kozono, J. White, P. Marrack, and J. Kappler. 1998. Detection of antigen-specific T cells with multivalent soluble class II MHC covalent peptide complexes. *Immunity*. 8:675–682. doi:10.1016/S1074-7613(00)80572-5

Falta, M.T., A.P. Fontenot, E.F. Rosloniec, F. Crawford, C.L. Roark, J. Bill, P. Marrack, J. Kappler, and B.L. Kotzin. 2005. Class II major histocompatibility complex-peptide tetramer staining in relation to functional avidity and T cell receptor diversity in the mouse CD4(+) T cell response to a rheumatoid arthritis-associated antigen. *Arthritis Rheum.* 52:1885–1896. doi:10.1002/art.21098

Fassò, M., N. Anandasabapathy, F. Crawford, J. Kappler, C.G. Fathman, and W.M. Ridgway. 2000. T cell receptor (TCR)-mediated repertoire selection and loss of TCR vβ diversity during the initiation of a $CD4^+$ T cell response in vivo. *J. Exp. Med.* 192:1719–1730. doi:10.1084/jem.192.12.1719

Ford, M.L., and B.D. Evavold. 2003. Regulation of polyclonal T cell responses by an MHC anchor-substituted variant of myelin oligodendrocyte glycoprotein 35-55. *J. Immunol.* 171:1247–1254.

Gebe, J.A., B.A. Falk, K.A. Rock, S.A. Kochik, A.K. Heninger, H. Reijonen, W.W. Kwok, and G.T. Nepom. 2003. Low-avidity recognition by CD4+ T cells directed to self-antigens. *Eur. J. Immunol.* 33:1409–1417. doi:10.1002/eji.200323871

Gronski, M.A., J.M. Boulter, D. Moskophidis, L.T. Nguyen, K. Holmberg, A.R. Elford, E.K. Deenick, H.O. Kim, J.M. Penninger, B. Odermatt, et al. 2004. TCR affinity and negative regulation limit autoimmunity. *Nat. Med.* 10:1234–1239. doi:10.1038/nm1114

Grossman, Z., and W.E. Paul. 1992. Adaptive cellular interactions in the immune system: the tunable activation threshold and the significance of subthreshold responses. *Proc. Natl. Acad. Sci. USA*. 89:10365–10369. doi:10.1073/pnas.89.21.10365

Homann, D., L. Teyton, and M.B. Oldstone. 2001. Differential regulation of antiviral T-cell immunity results in stable CD8+ but declining CD4+ T-cell memory. *Nat. Med.* 7:913–919. doi:10.1038/90950

Homann, D., H. Lewicki, D. Brooks, J. Eberlein, V. Mallet-Designé, L. Teyton, and M.B. Oldstone. 2007. Mapping and restriction of a dominant viral CD4+ T cell core epitope by both MHC class I and MHC class II. *Virology*. 363:113–123. doi:10.1016/j.virol.2006.12.025

Huang, J., L.J. Edwards, B.D. Evavold, and C. Zhu. 2007. Kinetics of MHC-CD8 interaction at the T cell membrane. *J. Immunol.* 179:7653–7662.

Huang, J., V.I. Zarnitsyna, B. Liu, L.J. Edwards, N. Jiang, B.D. Evavold, and C. Zhu. 2010. The kinetics of two-dimensional TCR and pMHC interactions determine T-cell responsiveness. *Nature*. 464:932–936. doi:10.1038/nature08944

Huppa, J.B., M. Axmann, M.A. Mörtelmaier, B.F. Lillemeier, E.W. Newell, M. Brameshuber, L.O. Klein, G.J. Schütz, and M.M. Davis. 2010. TCR-peptide-MHC interactions in situ show accelerated kinetics and increased affinity. *Nature*. 463:963–967. doi:10.1038/nature08746

Kersh, G.J., E.N. Kersh, D.H. Fremont, and P.M. Allen. 1998. High- and low-potency ligands with similar affinities for the TCR: the importance of kinetics in TCR signaling. *Immunity*. 9:817–826. doi:10.1016/S1074-7613(00)80647-0

Korn, T., J. Reddy, W. Gao, E. Bettelli, A. Awasthi, T.R. Petersen, B.T. Bäckström, R.A. Sobel, K.W. Wucherpfennig, T.B. Strom, et al. 2007. Myelin-specific regulatory T cells accumulate in the CNS but fail to control autoimmune inflammation. *Nat. Med.* 13:423–431. doi:10.1038/nm1564

Liu, G.Y., P.J. Fairchild, R.M. Smith, J.R. Prowle, D. Kioussis, and D.C. Wraith. 1995. Low avidity recognition of self-antigen by T cells permits escape from central tolerance. *Immunity*. 3:407–415. doi:10.1016/1074-7613(95)90170-1

Malherbe, L., C. Hausl, L. Teyton, and M.G. McHeyzer-Williams. 2004. Clonal selection of helper T cells is determined by an affinity threshold with no further skewing of TCR binding properties. *Immunity*. 21:669–679. doi:10.1016/j.immuni.2004.09.008

Mallone, R., S.A. Kochik, H. Reijonen, B. Carson, S.F. Ziegler, W.W. Kwok, and G.T. Nepom. 2005. Functional avidity directs T-cell fate in autoreactive CD4+ T cells. *Blood*. 106:2798–2805. doi:10.1182/blood-2004-12-4848

Mendel, I., N. Kerlero de Rosbo, and A. Ben-Nun. 1995. A myelin oligodendrocyte glycoprotein peptide induces typical chronic experimental autoimmune encephalomyelitis in H-2b mice: fine specificity and T cell receptor V beta expression of encephalitogenic T cells. *Eur. J. Immunol.* 25:1951–1959. doi:10.1002/eji.1830250723

Mendel, I., N. Kerlero de Rosbo, and A. Ben-Nun. 1996. Delineation of the minimal encephalitogenic epitope within the immunodominant region of myelin oligodendrocyte glycoprotein: diverse V beta gene usage by T cells recognizing the core epitope encephalitogenic for T cell receptor V beta b and T cell receptor V beta a H-2b mice. *Eur. J. Immunol.* 26:2470–2479. doi:10.1002/eji.1830261030

Moon, J.J., H.H. Chu, M. Pepper, S.J. McSorley, S.C. Jameson, R.M. Kedl, and M.K. Jenkins. 2007. Naive CD4(+) T cell frequency varies for different epitopes and predicts repertoire diversity and response magnitude. *Immunity*. 27:203–213. doi:10.1016/j.immuni.2007.07.007

Murali-Krishna, K., J.D. Altman, M. Suresh, D.J. Sourdive, A.J. Zajac, J.D. Miller, J. Slansky, and R. Ahmed. 1998. Counting antigen-specific CD8 T cells: a reevaluation of bystander activation during viral infection. *Immunity*. 8:177–187. doi:10.1016/S1074-7613(00)80470-7

Oxenius, A., M.F. Bachmann, P.G. Ashton-Rickardt, S. Tonegawa, R.M. Zinkernagel, and H. Hengartner. 1995. Presentation of endogenous viral proteins in association with major histocompatibility complex class II: on the role of intracellular compartmentalization, invariant chain and the TAP transporter system. *Eur. J. Immunol.* 25:3402–3411. doi:10.1002/eji.1830251230

Price, D.A., J.M. Brenchley, L.E. Ruff, M.R. Betts, B.J. Hill, M. Roederer, R.A. Koup, S.A. Migueles, E. Gostick, L. Wooldridge, et al. 2005. Avidity for antigen shapes clonal dominance in $CD8^+$ T cell populations specific for persistent DNA viruses. *J. Exp. Med.* 202:1349–1361. doi:10.1084/jem.20051357

Ronchese, F., M.A. Brown, and R.N. Germain. 1987. Structure-function analysis of the Abm12 beta mutation using site-directed mutagenesis and DNA-mediated gene transfer. *J. Immunol.* 139:629–638.

Sabatino, J.J., Jr., J. Shires, J.D. Altman, M.L. Ford, and B.D. Evavold. 2008. Loss of IFN-gamma enables the expansion of autoreactive CD4+ T cells to induce experimental autoimmune encephalomyelitis by a non-encephalitogenic myelin variant antigen. *J. Immunol.* 180:4451–4457.

Savage, P.A., J.J. Boniface, and M.M. Davis. 1999. A kinetic basis for T cell receptor repertoire selection during an immune response. *Immunity*. 10:485–492. doi:10.1016/S1074-7613(00)80048-5

Slifka, M.K., and J.L. Whitton. 2001. Functional avidity maturation of CD8(+) T cells without selection of higher affinity TCR. *Nat. Immunol.* 2:711–717. doi:10.1038/90650

Vollers, S.S., and L.J. Stern. 2008. Class II major histocompatibility complex tetramer staining: progress, problems, and prospects. *Immunology*. 123:305–313. doi:10.1111/j.1365-2567.2007.02801.x

Wasserman, H.A., and B.D. Evavold. 2008. Induction of anergy by antibody blockade of TCR in myelin oligodendrocyte glycoprotein-specific cells. *J. Immunol.* 180:7259–7264.

Weaver, C.T., A. Saparov, L.A. Kraus, W.O. Rogers, R.D. Hockett, and R.P. Bucy. 1998. Heterogeneity in the clonal T cell response. Implications for models of T cell activation and cytokine phenotype development. *Immunol. Res.* 17:279–302. doi:10.1007/BF02786452

Whitmire, J.K., N. Benning, and J.L. Whitton. 2006. Precursor frequency, nonlinear proliferation, and functional maturation of virus-specific CD4+ T cells. *J. Immunol.* 176:3028–3036.

Williams, M.A., E.V. Ravkov, and M.J. Bevan. 2008. Rapid culling of the CD4+ T cell repertoire in the transition from effector to memory. *Immunity*. 28:533–545. doi:10.1016/j.immuni.2008.02.014

Wooldridge, L., A. Lissina, D.K. Cole, H.A. van den Berg, D.A. Price, and A.K. Sewell. 2009. Tricks with tetramers: how to get the most from multimeric peptide-MHC. *Immunology*. 126:147–164. doi:10.1111/j.1365-2567.2008.02848.x

Zehn, D., and M.J. Bevan. 2006. T cells with low avidity for a tissue-restricted antigen routinely evade central and peripheral tolerance and cause autoimmunity. *Immunity*. 25:261–270. doi:10.1016/j.immuni.2006.06.009

Zehn, D., S.Y. Lee, and M.J. Bevan. 2009. Complete but curtailed T-cell response to very low-affinity antigen. *Nature*. 458:211–214. doi:10.1038/nature07657